

8654-EE-01

AD

**INVESTIGATION OF LOW FREQUENCY NOISE PROPERTIES OF
WIDE GAP SEMICONDUCTORS, SiC AND GaN, AND THE MAIN
PROPERTIES OF THE SiC BASED POWER DEVICES, DIODES AND
THYRISTORS**

Final Technical Report

by
M.E. LEVINSHTEIN

November 2000

United States Army

EUROPEAN RESEARCH OFFICE OF THE U.S. ARMY

London, England

CONTRACT NUMBER 68171-99-M-6802

20010523038

A.F. IOFFE INSTITUTE OF RUSSIAN ACADEMY OF SCIENCES

Approved for Public Release; distribution unlimited

AD NUMBER	DATE	DTIC ACCESSION CE
1. REPORT IDENTIFYING INFORMATION		REC
A. ORIGINATING AGENCY Institute of Russian Academy of Sciences, RU.		1. P or 2. Cc 3. AI r 4. U 5. L
B. REPORT TITLE AND/OR NUMBER Investigation of Low Noise Properties of wide gap semiconductors, SiC & GaN, & the Main Properties of the SiC Based Power Devices, Diodes & Thyristors C. MONITOR REPORT NUMBER RD 8654-EE-01		D1 1. 2.
D. PREPARED UNDER CONTRACT NUMBER N68171-99-M-6802		
2. DISTRIBUTION STATEMENT		
APPROVED FOR PUBLIC RELEASE		
DISTRIBUTION UNLIMITED		
FINAL		
DTI OCT 95		DITIONS ARE OBSOLETE

20010523038

REPORT DOCUMENTATION PAGE			Form Approved OMB No.0704-0188
1. AGENCY USE ONLY (Leave Blank)	2. REPORT DATE 09 Nov. 2000	3. REPORT TYPE AND DATES COVERED Final, October 1999 - November. 2000	
4. TITLE AND SUBTITLE INVESTIGATION OF LOW FREQUENCY NOISE PROPERTIES OF WIDE GAP SEMICONDUCTORS, SiC AND GaN, AND THE MAIN PROPERTIES OF THE SiC BASED POWER DEVICES, DIODES AND THYRISTORS		5. FUNDING NUMBERS	
6. AUTHOR(S) M.E. LEVINSHTEIN			
7. PERFORMING ORGANIZATION NAME(S) AND ADDRESS(ES) IOFFE INSTITUTE OF RUSSIAN ACADEMY OF SCIENCES 194021 ST. PETERSBURG, RUSSIA			8. PERFORMING ORGANIZATION REPORT NUMBER
9. SPONSORING/MONITORING AGENCY NAME(S) AND ADDRESS(ES) NAVAL REGIONAL CONTRACTING CENTER DETACHMENT LONDON, BLOCK 2, WING 11, EASTCOTE ROAD, RUISLIP, MIDDLESEX, HA4 8BS, ENGLAND, UK			10. SPONSORING/MONITORING AGENCY REPORT NUMBER
11. SUPPLEMENTARY NOTES			
12a. DISTRIBUTION/AVAILABILITY STATEMENT			12b. DISTRIBUTION CODE
13. ABSTRACT (Maximum 200 words) Low frequency noise properties of SiC, GaN, and SiC and GaN-based structures have been investigated. At elevated temperatures, the main contribution to low frequency noise in SiC structures comes from a surface local level. A method is proposed for extracting parameters of local surface levels in semiconductors from noise spectroscopic data. It has been shown that the level of flicker noise in GaN strongly depends on the structural perfection of the material. The nature of the 1/f noise in GaN can be similar to that in GaAs and Si. The 1/f noise is caused by the fluctuations of the occupancy of the tail states near the band edges. The systematic comparative investigation of the low frequency noise in GaN/GaAIN HEMTs has been provided in the temperature range $300 < T < 550$ K for the structures grown under identical conditions on sapphire and SiC substrates. The results obtained show that the level of 1/f noise is appreciably less for the samples on SiC substrates compared with those grown on sapphire. The Hooge parameter α for the wafers grown on SiC can be as small as $\alpha = 10^{-4}$. The effect of gate leakage current, surface states, levels in GaAIN, and noise channel on the total noise of GaAIN HFETs and MOS-HFETs has been investigated.			
14. SUBJECT ITEMS			15. NUMBER OF PAGES 25
			16. PRICE CODE
17. SECURITY CLASSIFICATION UNCLASSIFIED	18. SECURITY CLASSIFICATION UNCLASSIFIED	19. SECURITY CLASSIFICATION UNCLASSIFIED	20. LIMITATION OF ABSTRACT

ABSTRACT

Low frequency noise properties of SiC, GaN, and SiC and GaN-based structures have been investigated.

At elevated temperatures, the main contribution to low frequency noise in SiC structures comes from a surface local level. A method is proposed for extracting parameters of local surface levels in semiconductors from noise spectroscopic data.

It has been shown that the level of flicker noise in GaN strongly depends on the structural perfection of the material. The nature of the $1/f$ noise in GaN can be similar to that in GaAs and Si. The $1/f$ noise is caused by the fluctuations of the occupancy of the tail states near the band edges.

The systematic comparative investigation of the low frequency noise in GaN/GaN HEMTs has been provided in the temperature range $300 < T < 550$ K for the structures grown under identical conditions on sapphire and SiC substrates. The results obtained show that the level of $1/f$ noise is appreciably less for the samples on SiC substrates compared with those grown on sapphire. The Hooge parameter α for the wafers grown on SiC can be as small as $\alpha = 10^{-4}$.

The effect of gate leakage current, surface states, levels in GaN, and noise channel on the total noise of GaN HFETs and MOS-HFETs has been investigated.

LIST OF KEYWORDS

- Low frequency noise
- $1/f$ noise
- Generation-Recombination noise
- Wide-gap semiconductors
- Silicon Carbide (SiC)
- Gallium Nitride (GaN)
- Gallium-Aluminium Nitride (GaN)
- Field Effect Transistors (FETs)
- Heterostructure Field Effect Transistors (HFETs)

TABLE OF CONTENTS

1. STATEMENT OF THE PROBLEM

2. BACKGROUND

3. EXPERIMENTAL DETAILS

4. RESULTS AND ANALYSIS

4.1. Low frequency and $1/f$ noise in Silicon Carbide

4.2. Low frequency and $1/f$ noise in Gallium Nitride

4.3. Low frequency and $1/f$ noise in Gallium Aluminum Nitride and GaAlN HFETs

4.3.1. Low-frequency noise in AlGaN/GaN HFETs on SiC and sapphire substrates

4.3.2. Effect of gate leakage current on noise properties of AlGaN/GaN field effect transistors

4.3.3. Generation-Recombination Noise in GaN/GaAlN Heterostructure Field Effect Transistors

4.3.4. Noise in degenerated channel of HFETs

5. Conclusions and recommendations

1. Statement of the problem

The purpose of this work is to investigate the fundamental and most important practical aspects of the low frequency and $1/f$ noise in SiC, GaN, GaAlN-heterostructures, and devices based on these materials. SiC and III-nitride semiconductors have excellent potential for high temperature, high power, high frequency, and radiation hard applications. These two groups of materials are in the forefront of semiconductor research. Ultraviolet visible-blind photodetectors, blue and violet light emitting diodes, lasers, high voltage rectifier diodes, bipolar transistors, field-effect transistors of different types, thyristors, piezoelectric sensors have been fabricated using SiC and GaN/AlN/InN compounds.

Low frequency noise is one of the most important characteristics of any semiconductor material or device. This noise determines a lower limit of a signal level in broad-band circuits, controls the limiting detectivity of practically all types of photo-receivers. Low frequency noise is also one of the most important characteristics of devices used in microwave and optical communication systems. In certain cases, the low frequency noise can be used to control step-by-step the technological cycle of semiconductor device production and to control semiconductor device reliability. That is why the low frequency noise studies in SiC, GaN, and GaN/GaAlN heterojunctions are very important.

In this work we have studied:

- low frequency and $1/f$ noise in Silicon Carbide and 4H-SiC JFETs;
- low frequency and $1/f$ noise in Gallium Nitride (GaN);
- low frequency and $1/f$ noise in Gallium-Aluminum-Nitride and GaAlN HFETs, including comparative investigations of low-frequency noise in AlGaN/GaN HFETs made on SiC and sapphire substrates, effects of gate leakage current on noise properties of AlGaN/GaN FETs, Generation-Recombination (GR) noise in GaN/GaAlN HFETs, and noise in degenerated channels of HFETs.

2. Background

First measurements of low frequency noise in 6H-SiC [1] were performed in the space-charge limited current regime for the material of rather poor structural perfection. Only $1/f$ noise was observed in the material. The noise level in semiconductor materials and structures is usually characterized by the dimensionless Hooge parameter $\alpha = (S/I^2)/N$ [2], where N is the total number of the conduction electrons in the sample, f is the frequency of the analysis, S/I^2 is the relative spectral density of noise.

For one of the same semiconductor, the α values might differ by several orders of magnitude depending on the material structural perfection. For example, in Si and GaAs the values of α lie within the range $10^{-8} < \alpha < 10^{-2}$ [3,4]. A very high level of $1/f$ noise in 6H-SiC with the Hooge parameter $\alpha \approx 0.6$ was reported in Ref. [1].

The next measurement of the low frequency noise in n-type 6H-SiC was made after SiC technology had considerably improved [5]. This measurement demonstrated that in 6H-SiC with electron concentration $n = (1-2) \times 10^{17} \text{ cm}^{-3}$ in the temperature range from 300 to 600 K, the low frequency noise was a superposition of the $1/f$ noise and a single Lorenzian.

Low-frequency noise in 4H-SiC was investigated for the first time in Refs. [6,7]. A very low noise level was observed. At 300 K, the value of Hooge constant α was as small as $\sim 10^{-5}$, and the value of α decreased by appropriate annealing to $\alpha \approx 2 \times 10^{-6}$. After this annealing (at temperatures 500 - 600 K for several hours), the frequency dependence of the spectral noise density S had the form of the $1/f$ noise at $T < 500$ K [6]. Even this extremely low value of α was determined by the noise at the SiC-SiO₂ interface rather than by the bulk noise sources [6].

Even smaller noise level was observed in Ref. [8] for 4H-SiC JFET structures without the oxide layer. At 300 K, the values of the Hooge parameter were $\alpha = (2 \div 4) \times 10^{-6}$ at $f = 20$ Hz and $\alpha < 5 \times 10^{-7}$ at $f = 1300$ Hz. It has been concluded that the bulk $1/f$ noise was observed in these structures. In the temperature range $300 < T < 550$ K, the spectral density of bulk noise only weakly depended on the temperature. The frequency dependencies of the noise followed the law $S \sim 1/f^{1.5}$. At $T > 600$ K, the GR noise from a local level dominated in the low-frequency noise.

The capture cross section of electrons, σ was found to be strongly depended on temperature. Plotting the dependencies S_{\max} and $1/T_{\max}$ (see Fig. 3) versus $\ln f$ and using the technique suggested in Ref. [19] the main parameters of the level were determined [7]. Such analysis assumes that the level is positioned in the bulk of the SiC layer. The assumption of the temperature dependence of σ as $\sigma = \sigma_0 \exp(-E_1/kT)$ resulted in the unrealistic large σ_0 value of $\sim 10^{-1} \text{ cm}^2$.

First estimations of the low-frequency noise level in GaN were made in Refs. [9,10], where characteristics of visible-blind GaN p-n junction photodetectors were studied. Estimated α value was very high ($\alpha \approx 3$), although the noise equivalent power of the photodetectors was rather low ($6.6 \times 10^{-15} \text{ W/Hz}^{1/2}$ for $200 \times$

200 μm^2 photodetector). The results obtained with n-GaN resistors [11] confirmed these results. The temperature dependence of the noise was rather weak. The value of α is very large: $\alpha \approx 5 \div 7$. According to the theory [12], the level of 1/f noise should be correlated to the density-of-states in the tails near the bands boundaries. It is worth to note that the 1/f noise level and the density of states correlate also with the structural perfection of the semiconductor [13]. Hence these large α values manifest rather low level of the structural perfection of the material.

Low frequency noise in the frequency region from 20 Hz to 100 kHz was investigated in AlGaN/GaN HEMTs grown on SiC substrates [14]. Electron sheet concentration was equal to $1.5 \times 10^{13} \text{ cm}^{-2}$. It should be noted that electrons are degenerated at such high sheet concentrations [15]. The measured Hall electron mobility was $1400 \text{ cm}^2/\text{Vs}$ at 300 K. The noise spectra has the form of the 1/f (flicker) noise. The measured Hooge parameter is about $\sim 10^{-4}$. The possible contributions of the volume 1/f noise sources and the interface states at the GaN/AlGaN hetero-interface have been discussed [14].

3. Experimental Details

Low frequency noise in SiC has been investigated using 4H-SiC JFETs with a buried p⁺-n junction gate, manufactured by Cree Inc. The device design was basically the same as that reported earlier for 6H- and 4H-SiC JFETs [6]. The gate length L is 5 μm , gate width W is 1 mm. The doping density of the n-channel ($N_d - N_a = 2 \times 10^{17} \text{ cm}^{-3}$) was measured by the capacitance-voltage technique. At zero gate voltage $V_g = 0$, the thickness of the space-charge region on the p⁺-side is 0.1 μm . The active thickness of the channel determined from the pinch-off voltage is $t = 0.1 \mu\text{m}$ at $V_g = 0$. On the side opposite to the p⁺-gate, the channel is bounded either by an intentionally grown oxide or by the "free" surface of SiC. In the "oxide-free" devices, the magnitude of the 1/f noise within the temperature range $300 < T < 500 \text{ K}$ was essentially lower than the devices with an oxide layer on the surface. However, at $T > 500 \text{ K}$ the results for both types of devices were practically the same. All noise measurements were made at small drain-source biases V_{ds} (unsaturated regime) at $V_g = 0$. The spectral noise density S was found to be proportional to squared current $S \sim I^2$.

Low frequency noise in GaN has been investigated using 20-micron thick sample grown by hydride vapor phase epitaxy on sapphire. Sputtered ZnO was used as a buffer layer between the sapphire and GaN, but the ZnO was no longer present after completion of the growth. Except for a highly defective interface region of a few thousand angstroms thickness, the sample was of very high quality, with a 300-K mobility of $790 \text{ cm}^2/\text{Vs}$, and a carrier concentration of $1.28 \times 10^{17} \text{ cm}^{-3}$. Fits to the temperature-dependent Hall data in the bulk region yielded donor and acceptor concentrations of 2.1×10^{17} and $5 \times 10^{16} \text{ cm}^{-3}$, respectively, and a donor activation energy of 16 meV. The interface region, on the other hand, was strongly degenerate, with a sheet carrier concentration of $8 \times 10^{14} \text{ cm}^{-2}$ and an electron mobility of $55 \text{ cm}^2/\text{Vs}$. Further information on the electrical properties can be found in Ref. [16]. Ti (540 Å)-Al (1920 Å) contacts were deposited on the surface of the film and annealed at a temperature of 550°C for 2 min. The contact resistance, R_c , has been estimated using a transmission line model (TLM) measurements. Current-voltage characteristics measured between the contacts were linear and symmetrical with an accuracy of approximately 1%. The estimated contact resistance was approximately 1.9 Ohm.

Low frequency noise in AlGaN/GaN structures has been investigated using AlGaN/GaN HFETs grown by metal organic chemical vapor deposition on SiC and sapphire substrates using practically identical technology [17]. The 150 nm AlN layer grown on the substrate was followed by the deposition of a 1- μm nominally undoped GaN layer and a 50-nm n-GaN layer with estimated doping level between $2 \times 10^{17} \text{ cm}^{-3}$ and $5 \times 10^{17} \text{ cm}^{-3}$. The heterostructure was capped with a 40-nm Al_{0.2}Ga_{0.8}N barrier layer. The transistors had the source-drain spacing of 5 and 7 μm and the gate lengths, L , of 2, 3 μm , and 4, 5 μm , respectively. The gate widths, W , were 25, 50 and 75 μm . A low-frequency noise was measured in the frequency range from 1 Hz to 100 kHz in the temperature interval from 300 K to 550 K. The drain voltage fluctuations were measured in common source configuration at small values of the source-drain bias V_{ds} (linear, unsaturated regime). The probe station with the tungsten probes of 10- μm diameter and controlled pressure on the probes provided the contacts to the sample pads. Some transistors, both on SiC and sapphire substrates had a high gate leakage current. Gate currents were measured by a precision semiconductor analyzer HP 4156B.

4. Results and Analysis

4.1. Low frequency and 1/f noise in Silicon Carbide

As mentioned above, the level of 1/f noise in SiC at room temperature is rather small. However, at elevated temperatures $T > 500 \text{ K}$, the noise level increases strictly, and main contribution in the total noise comes from the local level. Because elevated temperatures are especially important for SiC and SiC-based

devices applications, the nature of the noise in this region is a "hot point" of the noise investigations for SiC [18].

Figure 1a shows the frequency dependencies of the spectral noise densities at different temperatures in 4H-SiC JFETs within the temperature range where the main contribution to the noise comes from the local level [7]. Fig. 1b shows the same data represented as S versus T dependencies at different frequencies f .

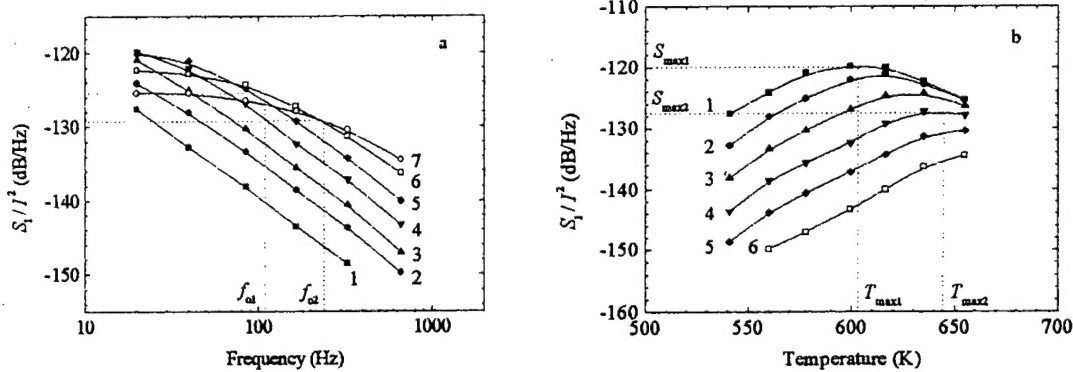


Fig. 1. Spectral noise density in 4H-SiC FET in linear regime at $V_g = 0$ [18]. (a) Data are presented as frequency dependencies of noise at different temperatures T (K): 1 - 541, 2 - 560, 3 - 578, 4 - 600, 5 - 617, 6 - 635, 7 - 655. (b) The same data are represented as temperature dependencies of noise at different frequencies f (Hz): 1 - 20, 2 - 40, 3 - 85, 4 - 165, 5 - 325, 6 - 660.

Very similar results have been obtained previously and analyzed with the assumption that the local bulk level is responsible for noise at elevated temperatures [7]. However, this approach leads, as pointed out in [7], to unrealistic results. An exponential temperature dependence of the capture cross section σ was assumed in [7]: $\sigma = \sigma_0 \exp(-E_1/kT)$, where E_1 is the activation energy. Although the calculated value of σ for the temperature of measurements was quite reasonable, the σ_0 value was unrealistically large ($\sim 10^{-1} \text{ cm}^2$).

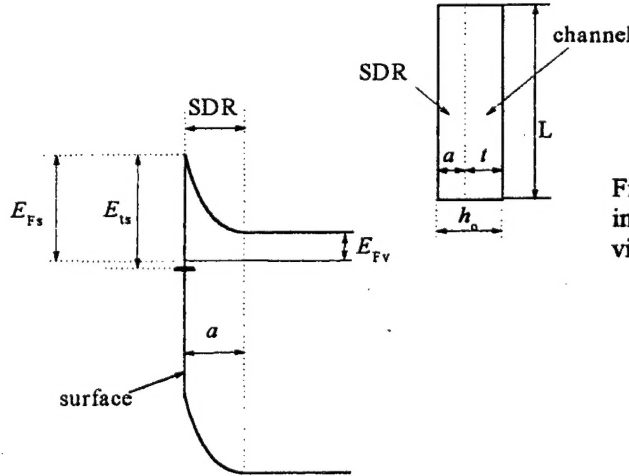


Fig. 2. Surface band diagram at the oxide/SiC interface. Inset shows schematically a cross-section view of the sample.

Let us consider the experimental data assuming that the level in question is located at the surface. A local level with concentration N_s and energy position E_s exists at the surface of a semiconductor structure. The sample has length L and width W (in the direction normal to the plane of Fig. 2), and a current I flows through the channel of thickness t (see inset in Fig. 2). On the left, the channel is bounded by the space charge region of thickness a , formed as a result of the presence of a surface charge (just the same geometry is realized in junction field-effect transistors in question).

Consider the situation when the concentration of the level, N_s , exceeds the total concentration of all other levels at the surface. Then just the level under consideration determines the position of the Fermi level at the surface, E_{Fs} (surface Fermi level pinning). The position of the Fermi level in the bulk, E_{Fv} , is determined by the doping level N_d and temperature T (Fig. 2). Assuming zero carrier concentration in the surface depletion region (SDR, Fig. 2), its width a can be found as

$$a = \left(\frac{2\epsilon\epsilon_0(E_{F_S} - E_{F_V})}{e^2 N_d} \right)^{1/2}, \quad (1)$$

where ϵ is the dielectric constant of the semiconductor, ϵ_0 is the permittivity of vacuum, and e is the electron charge. Fluctuations of the level occupancy cause fluctuations of the SDR width a :

$$\delta a = \frac{\delta n_{ts}}{N_d}, \quad (2)$$

where δn_{ts} is the fluctuation of the concentration of electrons trapped by the level. The fluctuations δa lead to fluctuations of the channel thickness $t = h_o - a$ and, consequently, to current fluctuations δI :

$$\frac{\delta I}{I} = -\frac{\delta n_{ts}}{N_d t}. \quad (3)$$

The relative spectral noise density of current fluctuations S/I^2 can be found as

$$S = \frac{S_I}{I^2} = 4 \cdot \frac{<(\delta I)^2>}{I^2} \cdot \frac{\tau}{1 + (\omega\tau)^2} = 4 \cdot \left(\frac{1}{N_d t} \right)^2 \cdot \frac{\tau}{1 + (\omega\tau)^2} \cdot <(\delta n_{ts})^2> \quad (4)$$

and

$$<(\delta n_{ts})^2> = \frac{N_{ts} F (1 - F)}{LW}, \quad (5)$$

where τ is the time constant associated with the return to equilibrium of the level occupancy, $\omega = 2\pi f$, and F is the occupancy of the level under consideration:

$$F = \frac{1}{1 + \exp\left(\frac{E_{F_S} - E_{ts}}{kT}\right)}. \quad (6)$$

Then Eq. (4) can be rewritten as

$$S = AF(1 - F) \cdot \frac{\tau}{1 - (\omega\tau)^2}, \quad (7)$$

where

$$A = \frac{4N_{ts}}{N_d^2 t^2 LW} = \frac{4N_{ts}}{N_o N_d t}$$

and $N_o = N_d t LW$ is the total number of the electrons in the channel.

The expression for the time constant τ follows from the Shockley-Hall-Read theory:

$$\tau = [C_n(n + n_1) + C_p(p + p_1)]^{-1}, \quad (8)$$

where $C_n = \sigma_n v_n$ and $C_p = \sigma_p v_p$ are the electron and hole capture probabilities; σ_n and σ_p are electron and hole capture cross sections; and v_n and v_p are the thermal velocities of electrons and holes. Using the usual approximation of zero free carrier concentration within the depletion region, ($n = p = 0$) and assuming that the level under consideration is located in the upper half of the forbidden gap ($C_n n_1 \gg C_p p_1$), the expression for τ can be rewritten as

$$\tau = \tau_0 \exp\left(-\frac{E_{ts}}{kT}\right), \quad (9)$$

where $\tau_0 = (\sigma_n v_n N_c)^{-1}$. Note that for a high enough concentration N_{ts} , the surface Fermi level E_{F_S} is practically pinned at the surface, and the occupancy of the level F depends on temperature weakly (this assumption was confirmed by direct numerical calculations, see below). Therefore, of all parameters appearing in Eq. (7) only τ strongly (exponentially) depends on temperature. This makes possible an analytical evaluation of all level parameters from the noise data. The technique of level parameters evaluation depends on the form of noise data presentation. Noise data are usually presented in two forms (see experimental curves in Figs. 1a and 1b):

- (i) spectral noise density S versus frequency f at different temperatures T (see Fig. 1a),
- (ii) S versus T at different f (see Fig. 1b).

In the case (i), one can directly obtain the time constant τ at a given temperature T , using the dependence $S(f)$:

$$\tau = \frac{1}{2\pi f_0}, \quad (10)$$

where f_o is the frequency at which the noise level is 3 dB (2 times) less than that at the plateau (Fig. 1a). At low frequencies $f(\omega\tau \ll 1)$, the spectral noise density S must be proportional to $\exp(E_{ts}/kT)$, all other values in Eq. (7) depending on temperature slightly:

$$S \sim \tau \sim \exp \frac{E_{ts}}{kT}. \quad (11)$$

Then, the slope of the S versus $\ln(1/kT)$ dependence (Arrhenius plot) gives the value of E_{ts} . On the other hand, for $\omega\tau \gg 1$

$$S \sim \frac{1}{\tau} \sim \exp \left(-\frac{E_{ts}}{kT} \right) \quad (12)$$

and again, the slope of the S versus $\ln(1/kT)$ plot gives the level position E_{ts} . With E_{ts} and τ known at a given temperature T , the capture cross section σ_n can be easily determined:

$$\sigma_n = \frac{\exp(\frac{E_{ts}}{kT})}{\tau N_c N_e}. \quad (13)$$

To find N_{ts} and F we have a system of two equations: Eq. (7) and equation of electroneutrality:

$$N_{ts} F = N_d a. \quad (14)$$

Assuming, as it was discussed before, that the Fermi level is pinned at the surface ($E_{Fv} \approx E_{ts}$), the value of a can be directly found from Eq. (1):

$$a \approx \left(\frac{2e\varepsilon_0 (E_{ts} - E_{Fv})}{e^2 N_d} \right)^{1/2}. \quad (15)$$

If the shallow donor impurities are fully ionized, the Fermi level in the volume E_{Fv} can be found as

$$E_{Fv} = kT \ln \frac{N_c}{N_d}. \quad (16)$$

where N_c is an effective density of states in the conduction band. Then

$$N_{ts} = \frac{(N_d a)^2}{N_d a - K}, \quad (17)$$

where

$$K = S L W \frac{1 + (\omega\tau)^2}{\tau} \left(\frac{N_d t}{2} \right)^2.$$

In the case (ii) the $S(T)$ dependencies may be used for theoretical analysis (see Fig. 1b). Of course, these two forms of noise data presentation are formally equivalent. However, the form (ii) is more "interference resistant". Characteristic maxima in $S(T)$ curves can be detected even when it is impossible to follow the behavior of the temperature dependence $\tau(T)$ over a wide range of temperatures for the first form of data presentation. To evaluate the local level parameters in the case (ii), the following procedure is proposed. Differentiating Eq. (7) with respect to $1/T$ and setting the derivative equal to zero, we have:

$$\frac{1}{kT_{max}} = -\frac{\ln \tau_o}{E_{ts}} - \frac{1}{E_{ts}} \ln \omega_m. \quad (18)$$

Hence, the slope of the plot of $1/kT_{max}$ against $\ln \omega$ yields the level position E_{ts} . With E_{ts} known, the time constant τ_o follows from (18):

$$\tau_o = \frac{1}{\omega_m} \exp \left(-\frac{E_{ts}}{kT_{max}} \right), \quad (19)$$

where $\omega_m = 2\pi f_m$ and f_m is the frequency at which $S = S_{max}$ at $T = T_{max}$. Substitution of Eq. (19) in Eq. (7) yields the value of S_{max} :

$$S_{max} = \frac{2}{N_d^2 t^2 \omega_m L W} N_{ts} F (1 - F). \quad (20)$$

Again, with E_{ts} used instead of E_{Fv} in Eq. (1), N_{ts} value can be found similarly to the case (i):

$$N_{ts} = \frac{2N_d a^2}{2a - S_{max} N_d t^2 \omega_m L W}. \quad (21)$$

Figure 3 shows $S(1000/T)$ dependencies for different frequencies of analysis, plotted using the data from Fig. 1a.

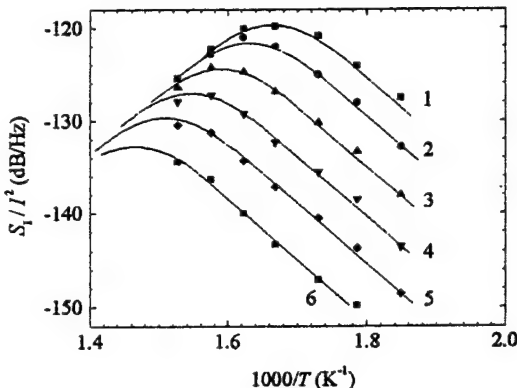


Fig. 3. Spectral noise density as a function of $1000/T$. The slope of $S(1000/T)$ gives the activation energy E_{ts} (see Eqs. (11) and (12)). Frequency of analysis f (Hz): 1 - 20, 2 - 40, 3 - 85, 4 - 165, 5 - 325, 6 - 660.

One can see, first of all, that at low temperatures, when the condition $\omega\tau \gg 1$ is fulfilled, the slope of the $S(1000/T)$ dependencies is the same for all the frequencies of analysis. On the other hand, for $f = 20$ Hz (curve 1 in Fig. 3) the slope of the $S(1000/T)$ dependence can also be found for high temperatures ($\omega\tau \ll 1$). It is seen that as it follows from Eqs. (11) and (12), the absolute values of the slopes for both high- and low-temperature parts of the curves in Fig. 3 are the same. The activation energy found from Fig. 3 $E_{ts} = 1.3$ eV. With $v_n \approx 2.4 \times 10^7$ cm/s and $N_c \approx 5.4 \times 10^{19}$ cm $^{-3}$ taken at $T = 650$ K, Eq. (13) yields $\sigma_0 \approx 10^{-14}$ cm 2 . The thickness of the SDR, a follows from Eqs. (15) and (16). At $T = 650$ K, $E_{Fv} = 0.31$ eV, and $a \approx 0.07$ μm for $N_d = 2 \times 10^{17}$ cm $^{-3}$. Then, the concentration N_{ts} can be calculated for any frequency and temperature from Eq. (17). The N_{ts} values fall within the range 10^{12} cm $^{-2} < N_{ts} < 2 \times 10^{12}$ cm $^{-2}$.

In Fig. 4, the dependence $1/kT_{\max}$ is plotted against $\ln\omega$ using data from Fig. 1b. According to Eq. (18), the slope of this plot gives the energy position of the level E_{ts} .

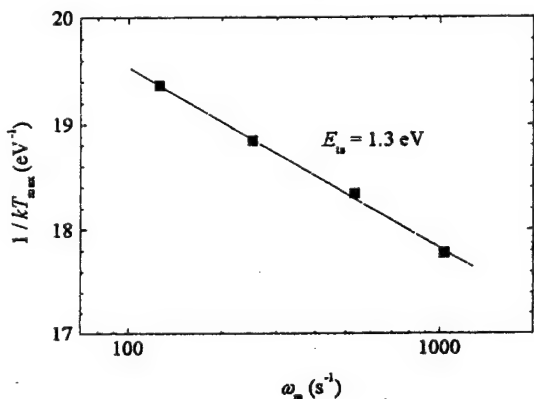


Fig. 4. $1/kT_{\max}$ versus $\ln\omega$, plotted using the data from Fig. 1b.

One can see that $E_{ts} = 1.3$ eV. Using Eq. (19), the value of capture cross-section $\sigma_0 = 1/\tau_0$ can be easily found. The calculated value of σ_0 is about 10^{-14} cm 2 , and calculated value of N_{ts} equals to $(1.5 - 2) \times 10^{12}$ cm $^{-2}$.

The approach proposed in this work is based on the assumption that the level occupancy F weakly depends on temperature. To support this assumption, a set of equations (1) and (14) was calculated numerically. In the temperature range of interest (600 K $< T < 660$ K), the occupancy of the level varies between 0.991 and 0.980. Note that at the same temperature interval, τ values vary by almost an order of magnitude, from 5.5×10^{-3} s to 6.8×10^{-4} s. Hence, the main assumption of the proposed approach seems to be correct.

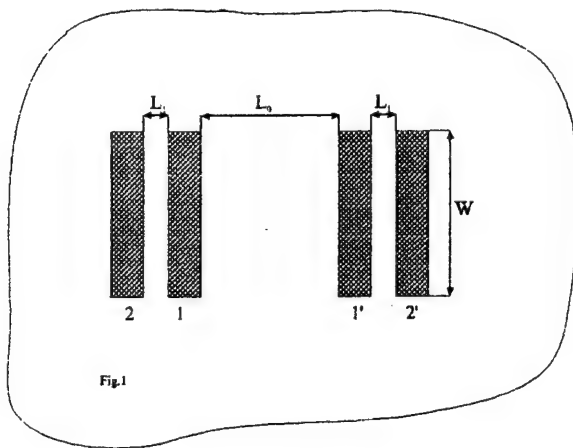
The level parameters found in this work from the noise data, are in good agreement with those obtained by other methods [19-21] for the SiC/SiO₂ interface. Therefore, there is a good reason to believe that the surface level at the SiC/SiO₂ interface is responsible for low frequency noise in 4H-SiC at elevated temperatures.

As discussed before, the noise properties at elevated temperatures are practically the same for the structures with native and intentionally grown oxide. Hence, one can conclude that the same surface states contribute to the noise in both types of structures.

The results obtained demonstrate the possibility of improving the noise properties of SiC structures at elevated temperatures by reducing the density of states at the SiC/SiO₂ interface.

4.2. Low frequency and $1/f$ noise in Gallium Nitride

As mentioned in Background, first estimates of the low-frequency noise level in n-GaN demonstrated very high values of Hooge parameter α values [9-11]. One might suggest several possible reasons for such a large $1/f$ noise level. The level of the $1/f$ noise is much higher for a semiconductor material with imperfections. Among other factors, a high dislocation density strongly increases the level of $1/f$ noise in certain cases [22,23]. The measured dislocation density in GaN samples grown on sapphire is of the order of $10^9 - 10^{10} \text{ cm}^{-2}$. On the other hand, theory [12] predicts that the level of $1/f$ noise should be proportional to the density of the tail states near the band edges. The density-of-states in the conduction band tail in GaN is much higher than that for Si and GaAs (see, for example [24]). Besides, for the samples used in [10,11], the electron mobility μ_n was approximately $60 \text{ cm}^2/\text{Vs}$ and was practically temperature independent in the range between 77 and 400 K.



To clarify the nature of the $1/f$ noise in GaN, we measured the low frequency noise in the samples grown on sapphire substrates with $\mu_n = 790 \text{ cm}^2/\text{Vs}$ at 300 K [25], and with the temperature dependence $\mu_n(T)$ close to that predicted by theory [26]. Low-frequency noise was measured between contacts 1 and 2, and 1 and 1' (see Fig. 5) in the dark and under band-to-band illumination. Current-voltage characteristics measured between the contacts were linear and symmetrical with an accuracy of approximately 1%. Resistance R_{12} between contacts 1 and 2 was equal to 9.85 Ohm; resistance R_{11} , between the contacts 1 and 1' was equal to 30.2 Ohm. The estimated contact resistance was approximately 1.9 Ohm for both configurations.

Figure 6 shows the frequency dependencies of the noise relative spectral density measured between the contacts 1 and 2.

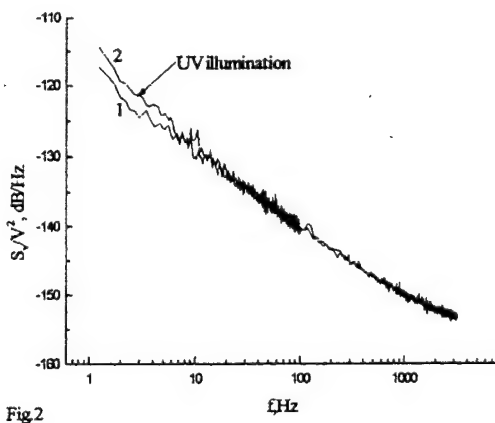


Fig.2

Fig. 6 Frequency dependencies of the current noise relative spectral density S_V/V^2 in the dark (Curve 1) and under band-to-band illumination (Curve 2) measured between contacts 1 and 2.

In the dark (Curve 1), the noise is typical $1/f$ (flicker) noise. The value of α calculated accordingly for the data presented in Fig. 6 is equal to $\approx 5 \times 10^{-2}$. This value is two orders of magnitude smaller than values of α in n-GaN reported earlier. Nevertheless, even this relatively low value of α is overestimated for two reasons. First, as usual for two-probe measurements, the contacts can give an essential contribution to the overall low-frequency noise [27]. Second, the obtained estimate is valid for a fully homogeneous current density distribution. However, in our case, the contacts penetrate into the GaN film not more than for a fraction of a micron.

Therefore, the current density j close to the contacts is substantially larger than the average current density across the sample. The noise spectral density S_v is proportional to j^4 [2]:

$$S_v = \frac{1}{I^2} \iiint \frac{\alpha \rho^2 j^4}{n f} dv, \quad (22)$$

where $\rho = 1/\sigma$ is the local resistivity, and n is the local electron concentration. The integral in Eq. (22) should be taken over the whole sample. Hence, the effective value of the total number of conduction electrons N in Eq. (1) (and, therefore, the value of α) should be less than the value of $N = LWtn_0$, used in the estimate for a homogeneous case. In fact, a relatively small region close to the contacts could make a dominant contribution to the $1/f$ noise.

Curve 2 in Fig. 6 presents the results under band-to-band illumination with an incandescent lamp. At a given illumination intensity, the photoconductivity $\sigma/\sigma_0 \approx 2 \times 10^{-2}$. The effect of the illumination is relatively weak. However the qualitative effect is quite similar to that for Si and GaAs [28]. The illumination has no effect at higher frequencies and increases the noise at relatively low frequencies.

Fig. 7 shows the frequency dependencies of the noise relative spectral density measured between the contacts 1 and 1'. The curve measured in the dark (Curve 1) has the form of $1/f$ noise (flicker) noise. Comparing Curves 1 in Figs. 6 and 7 one can see that the difference in the level of the dark noise is rather small for these two very different electrode configurations. The noise measured between contacts 1 and 1' should be considerably less than that between contacts 1 and 2.

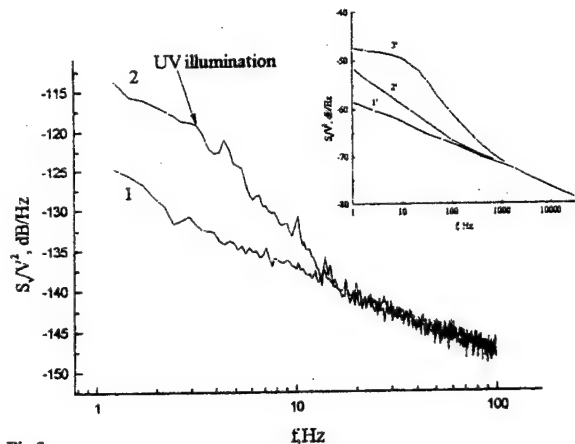


Fig.3

Fig. 7 Frequency dependencies of the current noise relative spectral density S_v/V^2 in the dark (Curve 1) and under band-to-band illumination. Inset shows the theoretical frequency dependencies of the noise spectral density under band-to-band illumination. $1' - b = 0$; $2' - b = 10^{-16}$; $3' - b = 10^{-15}$. Here b is a parameter which is approximately proportional to the illumination intensity [12].

It is clear that the total number of the conduction electrons involved is substantially smaller for the case represented in Fig 6 (contacts 1 and 2) compared to that shown in Fig. 7 (contacts 1 and 1') provided the metal contacts penetrated the whole depth of the film. A crude estimate for the expected noise level measured between contacts 1 and 1' can be obtained using the results obtained in Ref. [29]. According to these results, if the distance between the contacts L_o is much larger than the width of the contacts W ($L_o \gg W$, see Fig. 5), the rectangular contacts can be approximated by circular contacts with the effective radius $r_{\text{eff}} = W/4$. For such contacts (at $L_o \gg W$) the integral (2) can be evaluated.

It follows from such an evaluation that

$$\alpha = \frac{S_v}{V_o^2} \cdot f \cdot 16\pi^2 \cdot n_o \cdot r_{\text{eff}}^2 \cdot t \cdot \ln^2 \left(\frac{2L_o}{r_{\text{eff}}} \right), \quad (23)$$

where t is the thickness of the film, $r_{\text{eff}} = W/4$ (see Fig. 5), and V_o is the bias applied between the circular contacts. Comparing Eqs. (2) and (23) with $t = 20 \mu\text{m}$, $r_{\text{eff}} = 60 \mu\text{m}$, and $L_o = 1100 \mu\text{m}$, one can conclude that the flicker noise measured between contacts 1 and 1' at the same frequency f should be $\approx 25 \text{ dB}$ smaller. However, the measured difference in the noise levels is only $\approx 7 \text{ dB}$ (compare Curves 1 in Figs. 6 and 7). Once again, these results demonstrate that relatively small regions close to the surface contacts disproportionately contribute to the noise, and the deduced value of $\alpha \approx 5 \times 10^{-2}$ is only an upper bound for α . Curve 2 in Fig. 7 represents the results under band-to-band illumination. At a given illumination intensity, the photoconductivity $\sigma/\sigma_0 \approx 5 \times 10^{-3}$. Despite the fact that this photoconductivity is less than that for the case represented in Fig. 6, the effect of the band-to-band illumination is much stronger. Such an effect of band-to-band illumination on the $1/f$ noise was analyzed in details for Si samples in reference [30] using the model of $1/f$ noise developed in Ref. [12] (see the inset in Fig. 7).

The comparison of the observed effect of band-to-band illumination on the low-frequency noise (see Fig. 7) with the theory (see the inset) shows that the nature of the $1/f$ noise in GaN can be similar to that in GaAs and Si. The $1/f$ noise is caused by the fluctuations of the occupancy of the tail states near the band edges.

4.3. Low frequency and $1/f$ noise in Gallium Aluminum Nitride and GaAlN HFETs

4.3.1. Low-frequency noise in AlGaN/GaN HFETs on SiC and sapphire substrates

The available data on the α value in GaN/GaAlN heterostructures are quite contradictory. In particular, for GaN/GaAlN Heterojunction Field Effect Transistors (HFETs) grown on SiC substrates the values of α were found in the order of 10^{-4} [14]. In Ref. [27], the magnitude of the $1/f$ noise observed in GaN/GaAlN heterostructures grown on sapphire corresponds to the α values in the order of 10^{-2} . On the other hand, more recently, small values of $\alpha \sim 10^{-4}$ were reported for AlGaN/GaN HFETs grown on sapphire substrates [31,32]. The values of α for the same semiconductor might differ by several orders of magnitude depending on the material structural perfection. For example, in silicon and gallium arsenide the values of α lie within the range $10^{-8} - 10^{-2}$. In SiC the values of α are somewhat higher, $10^{-6} < \alpha < 1$. Studies of the low frequency noise in the samples grown on sapphire and SiC under identical conditions should allow us to compare the material quality of GaN on different substrates.

In Refs [33,34], we present the results of such studies for a large number of different AlGaN/GaN HFETs grown on sapphire and SiC substrates and fabricated using practically identical technology.

Fig. 8 presents the frequency dependencies of relative drain current spectral densities S/I_d^2 at $V_{ds} = 0.4$ V for different values of V_g . The inset shows the current voltage characteristics of the sample. One can see that at $V_{ds} = 0.4$ V, the transconductance is very small, and drain current depends very weakly on V_g : in the range of $0 < V_g < 0.8$ V, the drain current I_d changes from ~ 1.2 mA to ~ 0.92 mA, i.e. less than by 30 %. If the observed noise is due to the fluctuations of the contact resistance or to the surface noise of the structure, the expected change of the noise has to be less than 2 dB ($S_I \sim I_d^2$). If the main contribution to the observed noise comes from the channel resistance fluctuations, the expected change of noise level should be even less ($S_I \sim I_d$). However, the measured noise change was ≈ 15 dB. Hence, the measured noise is not caused by the contact or surface phenomena or by the channel resistance fluctuations. The only possible reason of the increase in the drain current fluctuations with the increase of the gate bias is the effect of the increased gate leakage current fluctuations to the output noise S/I_d^2 . This contribution can be essential even at very small I_g/I_d ratios: $I_g/I_d \leq 10^{-3} - 10^{-5}$. This result might be expected, since, in the structures under investigation, the gate leakage current flows through the AlGaN barrier layer with a large density of structural defects.

For the AlGaN/GaN devices with a low leakage current (and with low noise level of drain current), the results are similar to those reported for GaAs Metal-Semiconductor FETs (MESFETs) and AlGaAs/GaAs HEMTs, where the $1/f$ noise is nearly independent of the gate bias [35,36]. Only when the gate current increases sharply with a further gate voltage increase ($-V_g \geq 5.5$ V), S/I_d^2 .

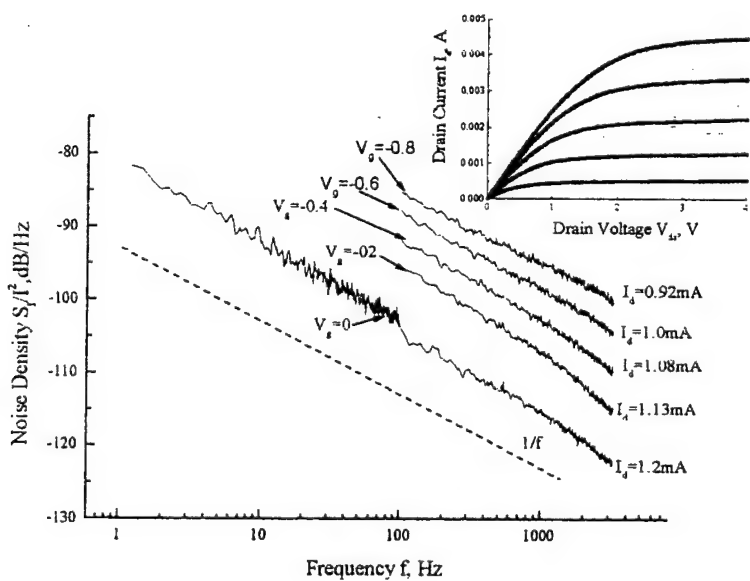


Fig. 8. Frequency dependencies of relative spectral noise density of drain current, I_d , for the sample with large leakage gate current (sample Sp2#2) at different gate biases, V_g . $V_{ds} = 0.4$ V. $T = 300$ K. Inset shows the output current-voltage characteristics of the sample at different values of V_g at 300 K. V_g (V): 1 - 0, 2 - 0.4, 3 - 0.8, 4 - 1.2, 5 - 1.6.

The studies of the mechanisms of the low frequency noise in FETs are usually performed at bias voltages corresponding to the linear regime of operation. However, in practical circuits, the transistors usually operate in saturation regime, at relatively high gate and drain voltages. The obtained results show that, for GaN/GaAIN HFETs, the I_g/I_d ratio at high biases should not exceed 10^{-6} - 10^{-5} for a low noise operation.

The frequency and temperature, and drain bias dependencies of the drain current noise, S_v/I_d^2 , measured on the samples with small gate leakage were nearly identical to the noise characteristics measured on similar gateless structures of the same geometry, for samples on both sapphire and SiC substrates. All further experiments were made using either gateless structures or the structures with small leakage current.

The results obtained show that the level of $1/f$ noise is appreciably less for the samples on SiC substrates compared with those grown on sapphire. The Hooge parameter α for the wafers grown on SiC can be as small as $\alpha = 10^{-4}$. This value of α is comparable to the α values for commercial GaAs MESFETs and only slightly higher than the typical values of α for Si n-channel MOSFETs. Table 1 lists the measured device parameters. Smaller values of α for the samples on SiC substrates correlate with a higher electron mobility in these samples compared with those grown on sapphire. A higher mobility and a lower noise level in the AlGaN/GaN heterostructures grown on SiC indicate their higher structural perfection compared with identical structures grown on sapphire.

The structures grown on SiC are characterized by a very weak temperature dependence of noise [33,34]. The very weak temperature dependence of the $1/f$ noise is very typical for the background $1/f$ noise in GaAs and SiC, where the measured $1/f$ noise was caused by the fluctuations in the occupancy of the levels that form the density of states tail near the conduction band edge. This weak temperature dependence of the low frequency noise in HFETs grown on SiC is advantageous for high temperature applications.

Table 1. Comparative noise data for the structures grown on sapphire and SiC substrates.

Sample	Hall mobility (cm^2/Vs)	Sheet density (cm^{-2})	Substrate
Sp1	1000	$(1.5\text{-}2) \times 10^{13}$	sapphire
Sp2	1220	7×10^{12}	sapphire
Sp3	1150	$(5\text{-}7) \times 10^{12}$	sapphire
SC1	1900	10^{13}	SiC
SC2	1400	1.5×10^{13}	SiC
SC3	1370	1.5×10^{13}	SiC

On contrary, the temperature dependencies of noise for the structures grown on sapphire indicate that, at $T > 320$ K, the main contribution to the noise comes from generation-recombination noise of local level. The slope of the appropriate Arrhenius plot determines the characteristic activation energy $\Delta E \approx 0.42$ eV. It is interesting to notice that the gate leakage current in GaN/GaAIN HFETs is temperature activated with the activation energy of 0.4 eV [37], which is very close to the activation energy extracted from the low frequency noise measurements.

Results obtained show that GaN/AlGaN heterostructures grown on SiC substrate have a lower level of $1/f$ noise and a higher electron mobility compared to samples grown on sapphire under identical conditions. The Hooge parameter, α , for the wafers grown on SiC can be as small as 10^{-4} . This value of α is comparable with the α value for commercial GaAs field effect transistors. The gate current noise might determine the total noise of the drain current I_d even at I_g/I_d ratios as small as 10^{-4} - 10^{-5} . For the structures grown on SiC, the low frequency noise is only weakly depends on temperature in the temperature range $300 < T < 550$ K. For devices grown on sapphire, the noise of a local level contributes to the overall low-frequency noise. The temperature dependence of the generation-recombination noise yielded the activation energy for this level, $E_a = 0.42$ eV.

4.3.2. Effect of gate leakage current on noise properties of AlGaN/GaN field effect transistors

The contribution of the gate leakage current fluctuations to the output drain current noise of AlGaN/GaN HFETs was studied by three different methods [38,39]. First, we studied the low frequency noise properties of the AlGaN/GaN HFETs and novel MOS-HFETs fabricated on the same wafer under identical conditions. The MOS-HFETs had an extremely low gate leakage current and the difference in gate current between HFETs and MOS-HFETs was several orders of magnitude. Second, the gate current fluctuations were measured directly, for the first time, in AlGaN/GaN HFETs. The appropriate analysis of the results also allowed us to calculate the contribution of gate current fluctuations to the output noise. Third, the correlation between the gate and drain current fluctuations were measured and analyzed.

Figure 9 shows the dependencies of the relative spectral noise density S_{ld}/I_d^2 on drain current for several HFETs and MOS-HFETs at constant drain voltage $V_d = 0.5$ V. For the devices from the first set of structures (on 4H-SiC insulating substrates) at high drain current ($V_g = 0$), the values of S_{ld}/I_d^2 are almost the same for both HFETs and MOS-HFETs. The noise level corresponded to the Hooge parameter $\alpha = (S_{ld}/I_d^2)Nf \approx 10^{-3}$. With a current decrease (i.e. at more negative gate voltages, V_g), the spectral noise density increased fairly rapidly for both the HFETs and MOS-HFETs. The difference in noise level between these two types of transistors increased with a decrease of the drain current and reached 7 - 8 dB at $I_d \approx 2 \times 10^{-3}$ A. However, this difference can not be explained by the contribution of the gate leakage current to the noise in HFETs. Indeed, the ratio I_g/I_d increases with a decreasing gate bias. Hence, the lower is the drain current, the higher should be the difference between noise in HFETs and MOS-HFETs. However at $I_d < 10^{-3}$ A, this difference becomes smaller, and at $I_d \sim 10^{-4}$ A, the noise is practically the same for the HFETs and MOS-HFETs. So, one can conclude that gate leakage current does not contribute to the output noise in the devices with the relatively high level of 1/f noise ($\alpha = 10^{-3}$).

Structures from the second set (conducting 6H-SiC substrate) were characterized by a low level of 1/f noise, which corresponded to the Hooge parameter $\alpha = 10^{-4}$. For these structures, spectral noise density S_{ld}/I_d^2 sharply increased with a drain current decrease (see the dashed line in Fig. 9).

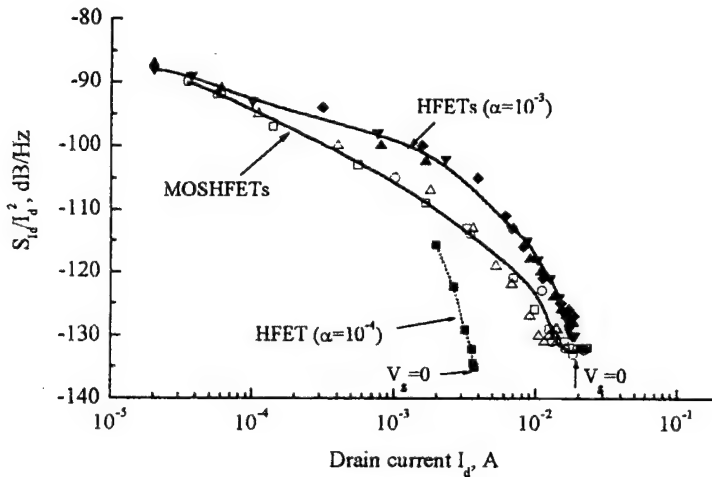


Fig. 9. Dependencies of the relative spectral noise density of drain current fluctuations S_{ld}/I_d^2 on drain current at constant drain voltage $V_d = 0.5$ V for the structures with "high" ($\alpha = 10^{-3}$, 4H-SiC insulating substrates) and "low" ($\alpha = 10^{-4}$, 6H-SiC conducting substrates) 1/f noise. Frequency of analysis $f = 200$ Hz.

When the drain current decreased by a factor less than two, the noise spectral density S_{ld}/I_d^2 increased by 20 dB for these devices. At the same time, for the high noise level devices, the noise increased by only 12 dB when the current changed from 2×10^{-2} A to 10^{-2} A. A rapid increase in noise was accompanied by a growth of a gate leakage current I_g . Note that at small drain current $I_d < 0.002$ A (large negative gate bias), the transistors from the second set demonstrated non-stable noise spectra which were not reproducible. Similar non-stationary behavior of the leakage current through the oxide is known for Si MOSFETs. Such a behavior can be considered as additional evidence that the gate leakage current fluctuations contribute to the output noise. To confirm these conclusions, the direct measurements of the gate current fluctuations have been performed.

The gate current is divided between drain and source in proportion, which depends on the gate-source and gate-drain biases and source and drain series resistances. The part of the gate current flowing to the drain gives an additive contribution to the output noise. The part of the gate current flowing to the source produces voltage fluctuations, which are amplified by the transistor.

In order to measure the gate current fluctuations, a small resistor R_g should be connected in series with the gate. If the entire gate current flows to the drain, the relative spectral noise density of drain current fluctuations due to the gate current fluctuations is given by:

$$\frac{S_{ld}}{I_d^2} = \frac{S_{Vg}}{R_g^2 I_d^2}, \quad (24)$$

where S_{Vg} is spectral noise density of gate voltage fluctuations.

If the entire gate current flows to the source, it produces the voltage fluctuations across source series contact resistance R_c and across a fraction of the channel resistance, R_{ch} . This resistance is on the order of $R_c + \beta R_{ch}$, where β is a parameter that depends on the gate current and is on the order of 0.2 to 0.5. In the linear regime, this resistance is close to a half of the output resistance $r = V_d/I_d$. Hence, the fluctuations of the drain current due to this mechanism can be estimated as:

$$\frac{S_{Id}}{I_d^2} = \frac{S_{Vg}}{R_g^2 I_d^2} \frac{r^2}{4} g^2, \quad (25)$$

where g is external transconductance in the linear region.

Figure 10 illustrates the possible contribution of gate current fluctuations to the output noise of the structures with relatively high level of $1/f$ noise (4H-SiC insulating substrate) and structures with low $1/f$ noise (6H-SiC conducting substrate). Curves labeled 1 in Figs. 10a and 10b show the measured dependencies of the drain current fluctuations S_{Id}/I_d^2 on the drain current. Symbols on curves 2 and 3 represent the contribution of the gate current fluctuations to the output noise for this structure calculated according to Eqs (24) and (25) respectively, using the experimental values of S_{Vg} , r , and g .

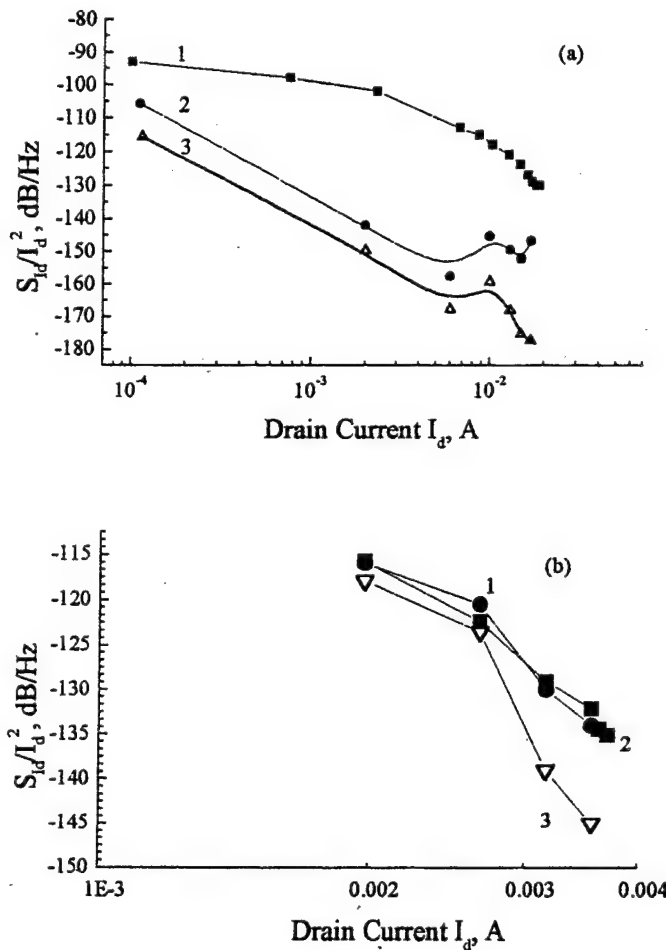


Fig. 10. Dependencies of the relative spectral noise density of drain current fluctuations S_{Id}/I_d^2 on drain current at constant drain voltage $V_d = 0.5V$. Frequency of analysis $f = 200$ Hz. (a)- high noise HFETs, (b) - low noise HFETs. Curves marked with (1) represent the experimental results. Symbols on the curves (2) and (3) represent the contribution of the gate current fluctuations to the output noise calculated according to Eqs. (24) and (25) respectively.

Eqs. (24) and (25) represent the upper bound for these two mechanisms of the gate leakage current contribution to noise. Therefore Fig. 10a shows that in the HFETs with relatively high level of $1/f$ noise, the gate leakage current fluctuations do not contribute much to the output noise.

As shown in Fig. 10b, fluctuations of gate current can cause the output noise in the low noise devices (on conducting 6H-SiC structures). The transistors on both insulating and conducting SiC had the gate leakage current of the same order of magnitude. However, the value of Hooge constant α for these devices differed by approximately one order of magnitude.

If the gate current fluctuations cause the HFETs output noise, drain and gate current fluctuations should be correlated. In order to measure the cross spectrum of gate and drain current fluctuations, the signals from the drain and gate resistors were fed to the two inputs of a differential amplifier, which produced either the sum $\delta V_{sum} = (\delta V_g + \delta V_d)$ or the difference $\delta V_{diff} = (\delta V_g - \delta V_d)$ of these signals. The cross spectrum S_{gd} and the correlation function γ can be found as

$$S_{gd} = \frac{S_{sum} - S_{diff}}{4}, \quad (26)$$

$$\gamma = \frac{S_{gd}}{\sqrt{S_{Vd}} \times \sqrt{S_{Vg}}}. \quad (27)$$

The external gate resistor, R_g , (connected in series with the gate) causes an additional correlation between gate and source current fluctuations, since the gate current fluctuations are transferred to the gate voltage fluctuations and therefore, are amplified by the transistor:

$$S_{Vd} = S_{Ig} \left(\frac{R_d r}{R_d + r} \right)^2 R_g^2 g^2, \quad (28)$$

where R_d is the resistance connected in series with the drain. If resistance R_g is high enough, the noise signals from the gate and drain should be fully correlated ($\gamma = 1$).

For the "high noise" HFETs, the correlation function γ is close to unity at $R_g = 10^4 \Omega$ and goes to zero with the decrease of resistance R_g . This proves once again that fluctuations of the gate current in these transistors do not contribute to the drain current fluctuations. In contrast, for "low noise" HFETs, γ remains fairly high ($\gamma = 0.4 - 0.8$) even as R_g approaches zero. We note that the dispersion between experimental points for these HFETs is quite large. One of the possible reasons for this phenomenon is a non-stationary behavior of the gate current, demonstrated for Si MOSFETs [13]. Hence, we conclude that in these HFETs, the fluctuations of the gate leakage current do significantly contribute to the output noise.

The difference in the noise behavior of two types of HFETs can be explained by the difference in the structural perfection of the AlGaN and GaN layers in different types of HFETs.

Hence we were able to show that in the GaN-based HFETs with a low $1/f$ noise, the gate current fluctuations can significantly contribute to the output noise. In the devices with a relatively high level of the $1/f$ noise, the contribution of the gate leakage current to the low frequency noise of drain current is fully masked by other noise mechanisms. Hence, we conclude that GaN MOS-HFETs with a high degree of structural perfection might potentially lead to the development of the transistors with ultra-low $1/f$ noise, since in these devices, the gate leakage current is suppressed by many orders of magnitude.

4.3.3. Generation-Recombination Noise in GaN/GaAlN Heterostructure Field Effect Transistors

Recently, the structures with rather low value of $\alpha = 10^{-4} - 10^{-5}$ were reported both on SiC and sapphire substrates. These values of α are comparable to the values of α for commercial GaAs MESFETs and for Si n-MOSFETs. Just like in GaAs and Si FETs, and GaAs/GaAlAs HFETs, the contribution of the local levels to the low-frequency noise can be observed in the structures with such low $1/f$ noise. The generation-recombination (GR) noise from a local level was reported for the first time in GaN/GaAlN HFETs in Ref. [34]. The temperature dependence of low-frequency noise revealed a contribution to the noise from a local level with the activation energy, E_a of approximately 0.42 eV in the structures grown on sapphire substrate. The levels with $E_a \approx 0.85$ eV for GaN/GaAlN HFETs on sapphire substrate and with $E_a = 0.20 - 0.36$ eV on SiC substrate were observed in Ref. [41] using noise spectroscopy technique. The origin of these levels was not clear.

We present new experimental data on the temperature dependencies of the low-frequency noise for two types of GaN/GaAlN HFETs: conventional HFETs and novel MOS-HFETs. These data reveal the contribution of the traps with activation energy of 0.8 - 1.0 eV to the low frequency noise [42,43].

Figure 11 shows the temperature dependencies of relative noise density of short circuit drain current fluctuations S_V/I^2 (I is the drain current at given temperature) for conventional AlGaN/GaN HFETs (a) and AlGaN/GaN MOS-HFETs (b) in the frequency range from 110 Hz to 3200 Hz. In the investigated frequency range $S_V/I^2(T)$ dependencies for both types of devices exhibited a broad maximum. The temperature of the maximum T_{max} , increases with frequency. The spectral density S_{max} corresponding to the maximum decreases with frequency. Such $S(T)$ dependencies are typical for the noise from local levels.

Figures 11a and 11b show the temperature dependence of noise for different transistors from the same wafer. It is seen that the amplitude of the noise and the position of the maxima differ from transistor to transistor. Comparing Fig. 11a,11b with Fig. 11c we can conclude that the difference in noise dependencies between HFETs and MOS-HFETs fabricated on the same wafer does not exceed the difference between the data for different HFETs.

The maxima on $S_V/I^2(T)$ dependencies are rather broad. For some transistors (see Fig. 11b) the shift of the maximum with the temperature is not seen for several frequencies. This makes possible only qualitative determination of the activation energy E_a . The slope of appropriate Arrhenius plots gives the estimate of the characteristic activation energy $E_a \approx 0.8 - 1.0$ eV. These energies are approximately the same for HFETs and MOS-HFETs. The difference in noise dependencies between HFETs and MOS-HFETs structures does not exceed the difference between the data for different HFETs samples.

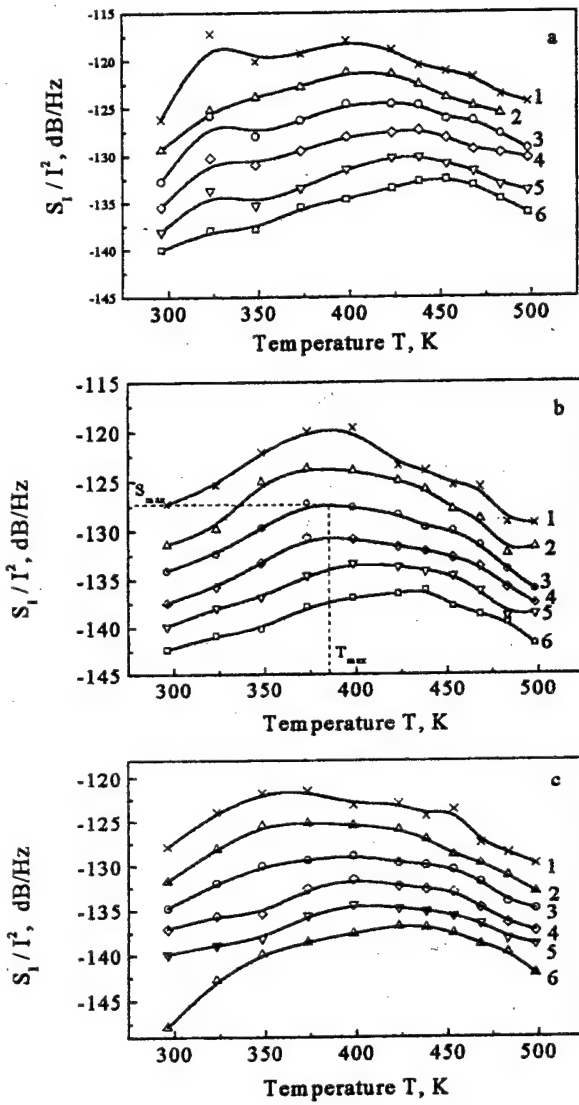


Fig. 11. Temperature dependencies of relative current noise density for conventional AlGaN/GaN HFETs (a), (b) and AlGaN/GaN MOS-HFETs (c) at different frequencies of analysis f . Frequency f (Hz): 1 - 110, 2 - 200, 3 - 400, 4 - 800, 5 - 1600, 6 - 3200 Hz. Gate voltage $V_g = 0$, drain-source voltage $V_{ds} = 0.5$ V.

It is clear, that the level observed in this paper can not be attributed to the gate leakage current I_g . The leakage current in AlGaN/GaN MOS-HFETs is negligible small. The characteristic value of I_g in such structures is less than 10 pA. The characteristic values of I_g for conventional GaN/GaAIN HFETs is four or more orders of magnitude higher. However, as can be seen from Fig. 11, the intensity of noise is approximately the same for the structures of both types.

Let us now analyze if the GR noise can originate from the traps located inside the channel.

For two dimensional (2D) case, the expression for relative spectral noise density S_I/I^2 generated by the single trap in the channel has the following form [44]:

$$\frac{S_I}{I^2} = \frac{4N_s}{L_0 W n_s} \frac{\tau F(1-F)}{1+(\omega\tau)^2}, \quad (29)$$

where N_s is the trap sheet concentration, L_0 and W are the channel length and width respectively, n_s is the electron sheet concentration, $\omega = 2\pi f$ is the circular frequency, $\tau = \tau_c F$ is the time constant associated with return to equilibrium of the occupation of the level, F is the Fermi - Dirac occupancy function, τ_c is the capture time constant

$$\tau_c = (\sigma n_s v_F)^{-1}, \quad (30)$$

where $v_F = (2E_F/m)^{1/2}$ is the electron velocity on the Fermi level.

For the 2D degenerate electron gas ($F \approx 1$), with the experimentally found value of τ , the capture cross section is:

$$\sigma \approx \frac{1}{m_s v_F}. \quad (31)$$

As shown in Ref. [7], $\tau(T_{\max}) = 1/2\pi f$. For $f = 400$ Hz ($\tau = 1/2\pi f = 8 \times 10^{-4}$ s $^{-1}$), and for $n_s = 1.2 \times 10^{13}$ cm $^{-2}$, we find:

$$E_F = \frac{\pi \hbar^2 n_s}{mkT} = 0.13 \text{ eV},$$

$v_F \approx 4.8 \times 10^7$ cm/s, and $\sigma \approx 3 \times 10^{-18}$ cm 2 (at $T = T_{\max} \approx 380$ K, see Figures 11a and 11b). This value of the capture cross section is too small to be realistic. This result shows that for degenerate 2D gas the source of low frequency generation-recombination noise, with any activation energy, can not be located directly in the 2D channel.

The generation - recombination noise observed can not also be explained by the tunneling of electrons from the 2D gas to GaN or AlGaN, because these processes do not require an activation energy.

Another possible location of the traps responsible for generation recombination noise is fully depleted GaAlN barrier layer (including GaAlN surface from the gate side). The GR noise from the traps in the AlGaN layer can be approximately described by Eq. (29), where N_t is replaced with $N_t d$. Here N_t is the volume concentration of traps and d is the thickness of the AlGaN. The time constant τ is now given by the Shockley-Hall-Read theory. Assuming zero free carrier concentration within the depletion region and that the level under consideration is located in the upper half of the forbidden gap, the expression for τ can be written as [45,46]:

$$\tau = \tau_0 \exp(E_t / kT), \quad (32)$$

where k is the Boltzmann constant, T is the temperature, $\tau_0 = (\sigma_n v_n N_c)^{-1}$, N_c is the density of states in the conduction band. Differentiating Eq. (29) with respect to $1/T$ and setting the derivative equal to zero, we find:

$$\frac{1}{kT_{\max}} = \text{const} - \frac{1}{E_t} \ln \omega. \quad (33)$$

Hence the slope of the plot of $1/kT_{\max}$ against $\ln f$ (Arrhenius plot) yields the level position E_t . From the slope of Arrhenius plots, we find the position of the level responsible for noise to be $E_a = E_t = 0.8 - 1.0$ eV. Once E_t is known, the time constant τ_0 can be found from Eq. (32):

$$\tau_0 = \frac{1}{\omega} \exp\left(-\frac{E_t}{kT_{\max}}\right) \quad (34)$$

and electron capture cross section of the level can be found as

$$\sigma_n = \frac{1}{\tau_0 v_n N_c}. \quad (35)$$

Taking for estimations the point in Fig. 11, where $\ln f = 6$ ($f = 400$ Hz), $T_{\max} = 384$ K the value of electron thermal velocity in $\text{Al}_{0.2}\text{Ga}_{0.8}\text{N}$ at 384 K $v_n = 2.6 \times 10^7$ cm/s, and density of state in the conduction band $N_c = 2.3 \times 10^{18}$ cm $^{-3}$, we find the electron capture section $\sigma_n \approx 10^{-12} - 10^{-13}$ cm 2 . This estimate for the capture cross section looks quite reasonable.

Figure 12 shows the $\ln S_{\max}$ versus $\ln f$ dependencies plotted for several samples of MOS-FETs and HFETs (see fig. 11 for the definition of S_{\max}).

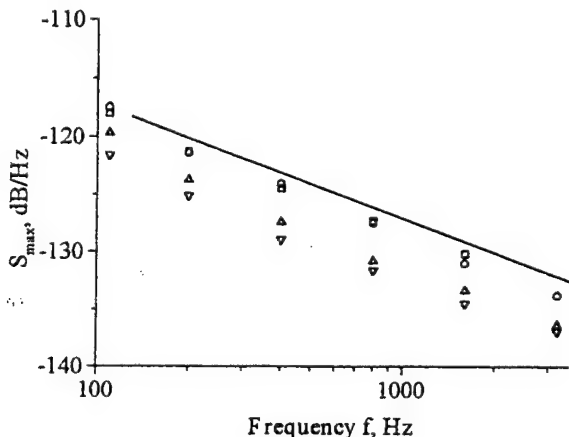


Fig. 12 The dependencies of S_{\max} versus $\ln f$ for different samples. The slope of the line is equal to unity.

It is seen that in all cases, the slope is equal to unity. Such kind of dependencies usually indicates that temperature dependence of noise is mainly determined by the temperature dependence of τ [18]. Then, the trap

concentration N_t can be crudely estimated as follows. Assuming that the main contribution to noise comes from the level with occupancy close to 0.5, we find for the trap concentration from Eq. (29)

$$N_t = \frac{4\pi f_{\max} S_{\max} n_s^2 L_0 W}{d}. \quad (36)$$

Taking $S_{\max} = -125$ dB/Hz, at $f = 400$ Hz we obtain $N_t \approx 5 \times 10^{16}$ cm⁻³.

Our measurements of the low frequency noise of GaN/GaAlN HFETs and MOS-HFETs on SiC substrates reveal the contribution to noise from a local level with activation energy $E_a \sim 0.8 - 1.0$ eV. The analysis shows that the trap responsible for the observed generation-recombination noise can be located in the AlGaN barrier layer.

4.3.4 Noise in degenerated channel of HFETs

It is generally accepted that the nature of 1/f noise in semiconductors is not universal. Depending on the semiconductor material, temperature, contact quality surface treatment, etc., the contact 1/f noise, the surface 1/f noise, the bulk 1/f noise caused by mobility fluctuations, or the 1/f noise caused by carrier number fluctuations might be dominant.

A phenomenological model of bulk 1/f noise in semiconductors has been proposed in Ref. [12]. This model is based on the assumption that the 1/f noise appears as a result of fluctuations of the level occupancy of the density-of-state tails near the conduction or valence band edges. The model has successfully explained non-monotonic dependencies of the 1/f noise on band-to-band illumination intensity in Si and GaAs, certain mechanisms of persistent photoconductivity, and the 1/f noise in GaAs and Si with deliberately introduced structural defects. Fluctuations of occupancy of the density-of-states tails might also explain the 1/f noise in bulk SiC [47] and in bulk GaN [27,48].

A model of bulk 1/f noise in semiconductors was developed in paper [12] only for non-degenerated case. Meantime, the study of low frequency and 1/f noise at high doping level and in the condition of low temperatures is now one of the most actual problems. At cryogenic temperatures, the strong degeneracy can be observed even at moderate doping level. On the other hand, with decreasing of size of modern semiconductor devices, the doping level increases according to the conventional scaling relations, and for the semiconductors with small electron mass (GaAs, for example) the conditions of degeneration can be fulfilled even at room temperature for the most high frequency microwave devices. Besides, condition of strong degeneration is always satisfied in the channels of GaAs/GaAlAs, GaN/GaAlN, and other Heterostructure Field Effect Transistors.

We proposed the model of the 1/f-like noise in degenerated case [49]. The results obtained have been compared with appropriate experimental results.

Theoretical analysis. We will analyze the degenerate semiconductor of n-type doped by shallow donor with a concentration of N_d . There is a tail of density of states $\rho(\varepsilon)$ falling exponentially inside the band gap:

$$\rho(\varepsilon) = \rho(0) \exp(-\varepsilon / \varepsilon_0), \quad (37)$$

where ε_0 is a constant characterizing the rate of fall of the density of states. Following multiphonon capture model, we will assume that

$$\tau(\varepsilon) = \tau(0) \exp(-\varepsilon / \varepsilon_1), \quad (38)$$

where $\tau(\varepsilon)$ is the time constant representing relaxation of the level occupancy (with a given energy ε) after deviation from equilibrium, ε_1 is the constant characterizing a reduction of the capture cross section on increase of level energy ε , $\tau(0) = \tau_0 F$ is appropriate constant at $\varepsilon = 0$ (at the boundary of the conduction band), τ_0 is the trapping time constant of the level at $\varepsilon = 0$, and

$$F = \frac{1}{1 + \exp(-\frac{\varepsilon_F - \varepsilon}{kT})}, \quad (39)$$

and

$$\varepsilon_F = \frac{(3\pi^2 n_0 \hbar^3)^{2/3}}{2m^*} \quad (40)$$

are the occupancy of the level of energy ε and the Fermi energy (m^* is the effective electron mass), respectively.

Let us select an energy interval $d\varepsilon$ at the depth ε within the density of state tail. Then the relative spectral noise density of electron number fluctuations $dS_n(\varepsilon)/n_0$ which appears as a result of the level occupancy fluctuations within the energy interval $d\varepsilon$ has the usual form:

$$\frac{dS_n(\varepsilon)}{n_0^2} = \frac{4\rho(\varepsilon)}{Vn_0^2} \frac{\tau(\varepsilon)F^2(1-F)}{1+(\omega\tau(\varepsilon))^2} d\varepsilon, \quad (41)$$

where V is the volume of the sample, $n_0 = N_d$ is a concentration of free electrons. The integration over all energies within the tail yield the spectrum noise density of carriers fluctuations:

$$\frac{S_n}{n_0^2} = \frac{4\tau_0 N_0}{Vn_0^2} \int_{-\infty}^0 \frac{F^2(1-F)e^{\varepsilon/\varepsilon_0 - \varepsilon/\varepsilon_1}}{1+\omega_0^2\tau_0^2 e^{-2\varepsilon/\varepsilon_1} F^2} \frac{d\varepsilon}{\varepsilon_0}, \quad (42)$$

where

$$N_0 = \int_{-\infty}^0 \rho(\varepsilon) d\varepsilon = \rho(0)\varepsilon_0$$

is the total density of levels in the tail. The upper limit of the integral (42) corresponds to the condition $\varepsilon_0 \ll \varepsilon_g$ (ε_g is the energy gap).

In degenerate case ($\varepsilon_F \gg kT$) the integral (42) can be taken analytically. At low frequencies $\omega\tau_0 \ll 1$, two cases should be considered. At $v = v_1 - v_0 < 1$, where $v_1 = kT/\varepsilon_1$ and $v_0 = kT/\varepsilon_0$

$$\frac{S_n}{n_0^2} = \frac{4N_0 kT \tau_0 e^{-\frac{\varepsilon_F}{kT}}}{Vn_0^2 \varepsilon_0 (v_0 + v_1 + 1)}. \quad (43)$$

One can see that in this case low frequency noise is frequently independent.

Just like in non-degenerate case [12], the most interesting case is encountered when $v > 1$, i.e. when the rise of time constant τ rapidly on increase in the level energy is more rapid than the fall of the density of states ($\varepsilon_1 < \varepsilon_0$). In this case

$$\frac{S_n}{n_0^2} = \frac{2N_0 \varepsilon_1 \tau_0 e^{-\frac{\varepsilon_F}{kT}}}{n_0^2 V \varepsilon_0} \frac{1}{(\omega\tau_0)^{\frac{v_1-v_0-1}{v_1}}} \frac{\pi}{\cos(\frac{\pi}{2} \frac{v_0+1}{v_1})} \sim \frac{1}{f^{\frac{v_1-v_0-1}{v_1}}}. \quad (44)$$

If $v \gg 1$, i.e. $\varepsilon_1 < \varepsilon_0$ and $\varepsilon_1 \ll kT$, the frequency dependence of the spectral noise density is of the pure $1/f$ type:

$$\frac{S_n}{n_0^2} = \frac{N_0 \varepsilon_1 e^{-\frac{\varepsilon_F}{kT}}}{n_0^2 V \varepsilon_0 f}. \quad (45)$$

The comparison with the corresponding formula for non-degenerate case [13] shows that the amplitude of the $1/f$ noise is suppressed in the degenerate case by a factor $\exp(-\varepsilon_F/kT)$. This results can be understand from simple physical considerations. As one can see from Eqs. (41) and (42), the intensity of the noise of the level is proportional to $F^2(1-F)$. For degenerate case, the occupancy function F is very close to unity for all levels in the forbidden gap, and $S \sim (1-F) \sim \exp(-\varepsilon_F/kT)$ (see Eq. (39)).

Comparison with the experiment. In Ref. [50], the $1/f$ noise was studied in GaAs epitaxial layers with doping level $N_d - N_a = (1 - 3) \times 10^{17} \text{ cm}^{-3}$ for temperatures 88 and 300 K. At 300 K, the electrons in GaAs with such a concentration are non-degenerated. The energy gap between the bottom of the conduction band ε_c and Fermi level ε_F is equal to $(\varepsilon_c - \varepsilon_F) \approx 0.022 \text{ eV}$, and $(\varepsilon_c - \varepsilon_F)/kT \approx 0.85$. At 88 K, electron gas is degenerated, and $(\varepsilon_F - \varepsilon_c)/kT \approx 1.9$. According to expressions obtained, one could expect decreasing of the $1/f$ noise level in ~ 20 times. Experimentally, the decreasing of about 100 times was observed. Evident tendency to sharp decreasing of the $1/f$ noise level when passing from non-degenerated to generated situation should be noted. On the other hand, quantitative difference between the prediction of the theory and the experimental results is observed. The temperature dependence of the capture cross sections of the levels which form the tale of density of states can make a contribution to the temperature dependence of the $1/f$ noise level. More detail experimental investigations should be provided to compare the prediction of the theory on the temperature dependence of the $1/f$ noise intensity.

Unusually small value of the $1/f$ noise was observed in degenerate GaAs of p-type in paper [51]. At room temperature, the smallest values of $\alpha \geq 10^{-4} - 10^{-5}$ are observed in pure low-doped samples of n-GaAs with doping level $N_d - N_a \sim 10^{14} - 10^{15} \text{ cm}^{-3}$ and high level of structural perfection. With doping level increasing, α usually increases. The α is equal to $10^{-4} - 10^{-5}$ for $N_d - N_a \sim 10^{16} \text{ cm}^{-3}$, and α is equal $10^{-3} - 10^{-2}$ for $N_d - N_a \sim 10^{17} \text{ cm}^{-3}$ [50, 52]. Such result is quite understandable because the density of state in the tails increases sharply with doping increase. The α value obtained in paper [51] for GaAs with the concentration of $N_a - N_d = 4 \times 10^{19} \text{ cm}^{-3}$ was equal to 3×10^{-5} . (The α value was not calculated in Ref. [51], however it can be easily made using the data on the geometrical sizes of the sample, doping level and noise data presented in [51]). One can believe that this small value of α is caused by the exponential decrease of the $1/f$ noise due to degeneration. Taking hole

effective mass in p-GaAs $m_p^* = 0.53m_e$ calculated magnitude of $(\varepsilon_v - \varepsilon_F)/kT = 3.1$ for $N_a - N_d = 4 \times 10^{19} \text{ cm}^{-3}$. As a result, the noise intensity is weakened by a factor $\exp(3.1) \approx 20$ times.

5. Conclusions and recommendations

The low frequency noise in 4H-SiC and 4H-SiC JFETs with buried p⁺-n junction gate has been studied within the temperature range from 300 to 660 K. At elevated temperatures, the main contribution to low frequency noise comes from a surface local level. A method is proposed for extracting parameters of local surface levels in semiconductors from noise spectroscopic data. Analytical expressions have been derived to calculate the energy position of the surface level in the forbidden gap, E_{ts} , capture cross section σ_n , and surface concentration N_{ts} . The parameters of the surface level responsible for the low frequency noise at elevated temperatures are found: $E_c - E_{ts} \approx 1.3 \text{ eV}$, $\sigma_n \sim 10^{-14} \text{ cm}^2$, $N_{ts} \approx 1.5 \times 10^{12} \text{ cm}^{-2}$.

The results obtained demonstrate the possibility of improving the noise properties of SiC structures at elevated temperatures by reducing the density of states at the SiC/SiO₂ interface.

Low-frequency noise in n-type gallium nitride (GaN) has been investigated. It was found that the noise spectra have the form of 1/f noise in the frequency range from 1 Hz to 100 kHz with a Hooge parameter α of approximately 5×10^{-2} . This value of α is two orders of magnitude smaller than that observed before in n-GaN. The obtained results show that the level of flicker noise in GaN strongly depends on the structural perfection of the material. The effects of band-to-band illumination on the low-frequency noise in GaN was successfully studied for the first time.

The results obtained show that the nature of the 1/f noise in GaN can be similar to that in GaAs and Si. The 1/f noise is caused by the fluctuations of the occupancy of the tail states near the band edges.

The systematic comparative investigation of the low frequency noise in GaN/GaAlN HEMTs has been performed in the temperature range $300 < T < 550$ K for the structures grown under identical conditions on sapphire and SiC substrates. The results obtained show that the level of 1/f noise is appreciably less for the samples on SiC substrates compared with those grown on sapphire. The Hooge parameter α for the wafers grown on SiC can be as small as $\alpha = 10^{-4}$. This value of α is comparable to the α values for commercial GaAs MESFETs and only slightly higher than the typical values of α for Si n-channel MOSFETs. A higher mobility and a lower noise level in the AlGaN/GaN heterostructures grown on SiC indicate their higher structural perfection compared with identical structures grown on sapphire.

The correlation between a transient behavior and 1/f noise in GaN/AlGaN Heterostructure Field Effect Transistors (HFETs) and novel GaN/AlGaN Metal-Oxide-Semiconductor Heterostructure Field Effect transistors (MOS-HFETs) has been investigated for the first time [53].

The contribution of the gate leakage current fluctuations to the output drain current noise of AlGaN/GaN HFETs was studied by different methods. In the devices with low level of the noise, the fluctuations of the gate leakage current I_g can give the main contribution to the output noise of the drain current I_g even at I_g/I_d ratio as small as $10^{-4} - 10^{-5}$. On the other hand, one can conclude that gate leakage current does not contribute to the output noise in the devices with the relatively high level of 1/f noise ($\alpha = 10^{-3}$).

It has been shown that GaN MOS-HFETs with a high degree of structural perfection might potentially lead to the development of the transistors with ultra-low 1/f noise, since in these devices, the gate leakage current is suppressed by many orders of magnitude.

The measurements of the low frequency noise of GaN/GaAlN HFETs and MOS-HFETs on SiC substrates reveal the contribution to noise from a local level with activation energy $E_a \sim 0.8 - 1.0$ eV. The analysis shows that the trap responsible for the observed generation-recombination noise can be located in the AlGaN barrier layer. Analytical theory has been proposed to analyze such kind of traps in GaN/GaAlN structures.

Analytical theory of the 1/f-like noise in degenerate semiconductors has been developed for the first time. This theory can be applied to estimate the contribution of the channel noise in total noise level on GaN/GaAlN structures.

The most actual problems in the field of low-frequency properties of wide-band semiconductors: SiC and GaN, and SiC and GaN-based structures can be formulated as follows:

- Decreasing the density of surface state at the SiC/SiO₂ boundary will allow to create SiC-based FETs with very low level of noise across whole temperature diapason from 300 to 700 K.
- The level of low-frequency noise in thin GaN films is defined by structure perfection of the epilayers.
- The low level of 1/f-like noise can be obtained in GaN/GaAlN structures both on SiC and sapphire substrates. In such low-noisy structures, the generation-recombination noise can make an essential contribution to total level of noise. The level of GR noise is defined by structure perfection of GaAlN layer.

The results obtained have been published in the following papers:

18. P.A. Ivanov, M.E. Levinshtein, J.W. Palmour, and S.L. Rumyantsev, *Semicond. Sci. Technol.*, 15 164 (2000).
25. S.L. Rumyantsev, D.C. Look, M.E. Levinshtein, M. Asif Khan, G. Simin, V. Adivarahan, R.J. Molnar, and M.S. Shur, *Proceedings of the International Conference on Silicon Carbide and Related Materials*. Research Triangle Park, North Carolina, USA, Oct. 10-15, 1999, p 1603.
33. S. Rumyantsev, M.E. Levinshtein, R. Gaska, M.S. Shur, J.W. Yang, and M.A. Khan., *Journ. Appl. Phys.*, 87, 1849 (2000).
34. S. Rumyantsev, M.E. Levinshtein, R. Gaska, M.S. Shur, A. Khan, J.W. Yang, G. Simin, A. Ping and T. Adesida, *Proceedings of the Third International Conference on Nitride Semiconductors (ICNS3)*, held in Montpellier, France in July 1999. *Phys. stat. sol. (a)*, 176 201 (1999).
38. S.L. Rumyantsev, N. Pala, M.S. Shur ,R. Gaska, M.E. Levinshtein, M. Asif Khan, G. Simin, X. Hu, and J. Yang, Accepted for publication in *Journal of Applied Physics*, Provisionally scheduled to N 12, 2000 (December 01).
39. S.L. Rumyantsev, N. Pala, M.S. Shur, M.E. Levinshtein, R. Gaska, X. Hu, J. Yang, G. Simin, and M. Asif Khan, *Techn. Digest, Intern. Workshop on Nitride Semicond., IWN2000*, Sept. 24 - 27, 2000, Nagoya, Japan, p. 128.
42. S.L. Rumyantsev, N. Pala, M.S. Shur, E. Borovitskaya, A.P. Dmitriev and M.E. Levinshtein R. Gaska, M. Asif Khan, J. Yang, X. Hu, and G. Simin, Accepted for publication in the Special Issue of *IEEE Trans. on Electron Devices* (July 2000).
43. S. Rumyantsev, M. Levinshtein, N. Pala, M. S. Shur, R. Gaska, A. Khan, S. Simin, and J. Yang, Presentation on *2000 Electronic Materials Conference*, Univ. of Denver, Colorado, June 21-23, 2000.
49. A.P. Dmitriev, E. Borovitskaya, M.E. Levinshtein, S.L. Rumyantsev, and M. S. Shur, Submitted for publication in *Journal of Applied Physics* (September 2000).
53. S.L. Rumyantsev, M.S. Shur, R. Gaska, X. Hu, A Khan, G. Simin, J. Yang, N. Zhang, S. DenBaars, and U.K. Mishra, *Electronics Letters*, 36, 757 (2000).

Literature Cited

1. S. Tehrani, L.L. Hench, C.M. Van Vliet, and G.S. Bosman, *J. Appl. Phys.*, **58**, 1571 (1985).
2. F.N. Hooge, T.G.M. Kleinpennings, and L.K.J. Vandamme, *Rep. Progr. Phys.*, **44**, 479 (1981).
3. R.H. Clevers, *Physica B*, **154**, 214 (1989).
4. F.N. Hooge and M. Tacano, *Physica B*, **190**, 145 (1993).
5. M.E. Levenshtein, S.L. Rumyantsev, and J.W. Palmour, *Techn. Phys. Lett.*, **19**, 513 (1993).
6. J.W. Palmour, M.E. Levenshtein, S.L. Rumyantsev, and G.S. Simin, *Appl. Phys. Lett.*, **68**, 2669 (1996).
7. M.E. Levenshtein, S.L. Rumyantsev, J.W. Palmour, and D.B. Slater, Jr., *Journ. Appl. Phys.*, **81**, 1758 (1997).
8. P.F. Flatresse and T. Ouisse, *Solid State Electron.*, **38**, 971 (1995).
9. A. Osinsky, S. Gangopadhyay, R. Gaska, B. Williams, M.A. Khan, D. Kusenkov, and H. Temkin, *Appl. Phys. Lett.*, **71**, 2334 (1997).
10. D.V. Kusenkov, H. Temkin, A. Osinsky, R. Gaska, and M. Khan, *Journ. Appl. Phys.*, **83**, 2142 (1998).
11. N.V. Dyakonova, M.E. Levenshtein, S. Contreras, W. Knap, B. Beaumont, and P. Gibart, *Semiconductors*, **32**, 257 (1998).
12. N.V. Dyakonova and M.E. Levenshtein, *Sov. Phys. Semicond.*, **23**, 175 (1989).
13. M.E. Levenshtein and S.L. Rumyantsev, *Sov. Phys. Semicond.*, **24**, 1125 (1990).
14. M.E. Levenshtein, S.L. Rumyantsev, R. Gaska, J.W. Yang, M.S. Shur, *Appl. Phys. Lett.*, **73**, 1089 (1998).
15. M.S. Shur, B. Gelmont, and M. Asif Khan, *J. Electronic Materials*, **25**, 777 (1996).
16. D.C. Look and R.J. Molnar, *Appl. Phys. Lett.*, **70**, 3377 (1997).
17. R. Gaska, A. Osinsky, J. Yang, and M. S. Shur, *IEEE Electron Device Letters*, **19**, 89 (1998).
18. P.A. Ivanov, M.E. Levenshtein, J.W. Palmour, and S.L. Rumyantsev, *Semicond. Sci. Technol.*, **15**, 164 (2000).
19. P.A. Ivanov, V.N. Panteleev, T.P. Samsonova, and V.E. Chelnokov, *Semiconductors*, **29**, 135 (1995).
20. P.A. Ivanov, K.I. Ignat'ev, V.N. Panteleev, and T.P. Samsonova, *Tech. Phys. Lett.*, **23**, 798 (1997).
21. M. Sadeghi, B. Liss, E.O. Sveinbjornsson and O. Engstrom, in *Silicon Carbide, III-Nitrides and Related Materials, part 2*, ed. G. Pensl, H. Monemar, and E. Janzen, Trans. Tech. Publ. LTD (Switzerland, Germany, UK, USA) p. 981 (1998).
22. A.M. Svetlichnyi, L.A. Koledov, V.V. Zotov, and E.F. Uvarov, *Sov. Phys. Semicond.*, **14**, 345 (1980).
23. V.M. Vinokur and S. P. Obukhov, *ZhETF*, **95**, 223 (1989).
24. O. Ambacher, W. Rieger, P. Ansmann, H. Angerer, T.D. Moustakas and M. Stutzman, *Sol. State Comm.*, **97**, 365 (1996).
25. S.L. Rumyantsev, D.C. Look, M.E. Levenshtein, M. Asif Khan, G. Simin, V. Adivarahan, R.J. Molnar, and M.S. Shur, *Proceedings of the International Conference on Silicon Carbide and Related Materials*, Research Triangle Park, North Carolina, USA, Oct. 10-15, 1999, p 1603.
26. D.C. Look, *Materials Sciences and Engineering*, **B50**, 50 (1997).
27. M.E. Levenshtein, F. Pascal, S. Contreras, W. Knap, S.L. Rumyantsev, R. Gaska, J.W. Jang, and M.S. Shur, *Appl. Phys. Lett.*, **72**, 3053 (1998).
28. N.V. Dyakonova, M.E. Levenshtein, and S.L. Rumyantsev, *Sov. Phys. Semicond.*, **25**, 1241 (1991).
29. Ollendorf Fr., *Erdstrome*, Russian Edition: Moscow-Leningrad, 1932.
30. N.V. Dyakonova, M.E. Levenshtein, D.L. Plotkin and S.L. Rumyantsev, *Sov. Phys. Semicond.*, **24**, 527 (1990).
31. A. Balandin, S. Cai, R. Li, K.L. Wang, Vol. Ramgopal Rao, and C.R. Viswanathan, *IEEE Electron Dev. Lett.*, **19**, 475 (1998).
32. J.A. Garrido, F. Calle, E. Munoz, I. Izpura, J.L. Sanches-Rojas, R. Li, and K.L. Wang, *Electron. Lett.*, **34**, 2357 (1998).
33. S. Rumyantsev, M.E. Levenshtein, R. Gaska, M.S. Shur, J.W. Yang, and M.A. Khan, *Journ. Appl. Phys.*, **87**, 1849 (2000).
34. S. Rumyantsev, M.E. Levenshtein, R. Gaska, M.S. Shur, A. Khan, J.W. Yang, G. Simin, A. Ping and T. Adesida, *Proceedings of the Third International Conference on Nitride Semiconductors (ICNS3)*, held in Montpellier, France in July 1999. *Phys. stat. sol. (a)*, **176** 201 (1999).
35. L.K.J. Vandamme, D. Rigaud, Jean-Marie Peransin, Robert Alaberda, and Jean-Michel Dumas, *IEEE Trans. Electron. Dev.*, **35**, 1071 (1988).
36. L.K.J. Vandamme, D. Rigaud, and Jean-Marie Peransin, *IEEE Trans. Electron. Dev.*, **39**, 2377 (1992).
37. R. Gaska, Q. Chen, J. Yang, A. Osinsky, M. Asif Khan, M.S. Shur, *IEEE Electron Device Letters*, **18**, 492 (1997).
38. S.L. Rumyantsev, N. Pala, M.S. Shur, R. Gaska, M.E. Levenshtein, M. Asif Khan, G. Simin, X. Hu, and J. Yang, Accepted for publication in *Journal of Applied Physics*, Provisionally scheduled to N 12, 2000 (December 01).

39. S.L. Rumyantsev, N. Pala, M.S. Shur, M.E. Levenshtein, R. Gaska, X. Hu, J. Yang, G. Simin, and M. Asif Khan, *Techn. Digest, Intern. Workshop on Nitride Semicond.*, IWN2000, Sept. 24 - 27, 2000, Nagoya, Japan, p. 128.
40. E. Simoen and C. Claes, *Semicond. Sci. Techn.*, 14, R61-R71 (1999).
41. A.Balandin, R. Li, S. Cai, J.Li, K.L. Wang, E.N. Wang, and M. Wojtowicz, *Proceedings of the 41st Electronic Materials Conference* (Univ. of California, Santa Barbara, California, 1999), p. 29.
42. S.L. Rumyantsev, N. Pala, M.S. Shur, E. Borovitskaya, A.P. Dmitriev and M.E. Levenshtein R. Gaska, M. Asif Khan, J. Yang, X. Hu, and G. Simin, Accepted for publication in the Special Issue of *IEEE Trans. on Electron Devices* (July 2000).
43. S. Rumyantsev, M. Levenshtein, N. Pala, M. S. Shur, R. Gaska, A. Khan, S. Simin, and J. Yang, Presentation on 2000 *Electronic Materials Conference*, Univ. of Denver, Colorado, June 21-23, 2000.
44. J.A. Copeland, *IEEE Trans. Electron Devices*, 18, 50 (1971).
45. P.O. Lauritzen, *Solid State Electron.*, 8, 41 (1965).
46. L.D. Yau and C.T. Sah, *IEEE Trans. on Electron. Dev.*, 16, 170 (1969).
47. M.E. Levenshtein, S.L. Rumyantsev, and J.W. Palmour, *Semicond. Sci. and Technol.*, 9, 2080 (1994).
48. M.E. Levenshtein, S.L. Rumyantsev, D.C. Look, R.J. Molnar, M. Asif Khan, G. Simin, V. Adivarahan, and M.S. Shur, *Journ. Appl. Phys.*, 86, 5075 (1999).
49. A.P. Dmitriev, E. Borovitskaya, M.E. Levenshtein, S.L. Rumyantsev, and M. S. Shur, Submitted for publication in *Journal of Applied Physics* (September 2000).
50. M.E. Levenshtein and S.L. Rumyantsev, *Techn. Phys. Lett.*, 19, 247 (1993).
51. F. Pascal, S. Jarrix, S. Delseney, G. Lecoy., and T. Kleinpennig, *Journ. Appl. Phys.*, 79, 3046 (1996).
52. M. Tacano and Y. Sugiyama, *IEEE Trans. on Electron Dev.*, 38, 2548 (1991).
53. S.L. Rumyantsev, M.S. Shur, R. Gaska, X. Hu, A Khan, G. Simin, J. Yang, N. Zhang, S. DenBaars, and U.K. Mishra, *Electronics Letters*, 36, 757 (2000).

ANNEX

**Amount of unused funds remaining on the contract at the
end of the period covered by report:**

\$6,250.00